ECS Transactions, 2 (12) 3-14 (2007)
10.1149/1.2408948, copyright The Electrochemical Society

Synthesis And Characterization Of A New Porphyrin-Fullerene Dyad Containing A β-Pyrrolic Linkage.

P. Tagliatesta[a], D. M. Guldi[b], and A. Lembo[a]

[a] Dipartimento di Scienze e Tecnologie Chimiche Università di Roma "Tor Vergata", Via Della Ricerca Scientifica, 00133 Rome, Italy.
[b] Institute for Physical Chemistry, Friedrich-Alexander University Erlangen-Nürberg, Egerlandstrasse 3, 91058 Erlangen Germany.

Two new β-substituted arylethynyl *meso*-tetraphenylporphyrins, 2-[(4'-formyl)phenyl]ethynyl-5,10,15,20-tetraphenylporphyrin (System A) and 2-[(4'-methyl)phenyl]ethynyl-5,10,15,20-tetraphenylporphyrin (System B) and their zinc derivatives were synthesized. Comparative UV/Visible and cyclic voltammetry studies of such macrocycles reveal the presence of an extensive conjugation between the tetrapyrrolic ring and the linker, through π–π orbitals interaction. This interaction was observed in form of a "push-pull" effect that moves the electronic charge between the porphyrin and the aldehyde group of the System A. System B, bearing a methyl instead of the formyl group, was synthesized in order to evaluate the effect of the substitution on the charge delocalization, which is necessary to corroborate the push-pull mechanism hypothesis. The new porphyrin, System A, was also used as starting material for the synthesis of new porphyrin-fullerene dyads in which the [60]fullerene is directly linked to the tetrapyrrolic rings by ethynylenphenylen subunits. Fluorescence and transient absorption measurements of the new dyads reveal that ultrafast energy and electron transfer occur respectively in non polar and polar solvents, with high values of the rate constant.

Introduction

The design of systems for the artificial light conversion and carbon dioxide reduction focuses on the long-term scientific challenge of mimicking the natural process by artificial means. In particular, such research attempts to replicate the natural process of photosynthesis, converting sunlight and carbon dioxide into carbohydrates and oxygen (1). Working on a better understanding of the detailed mechanisms of the photosynthetic process that provides and transfers electrons and energy led to employment of porphyrins and fullerenes.

In general, the two basic building blocks (i.e., porphyrins and fullerenes) are brought together through two different strategies – by self-assembly or by covalent bond formations that yield well-defined architectures (2,3). In most of the investigated architectures, porphyrins and fullerenes are organized into linear, 1-dimensional or 2-dimensional arrays (4), in which C_{60} is, however, covalently linked to the porphyrin *meso*-phenyl ring. Up to this point, there are only a few reports that describe the linkage of C_{60} to the tetrapyrrolic rings (5).

In the current presentation, we wish to present a series of newly β-substituted porphyrins – see Figure 1 –. UV/visible, NMR, and cyclic voltammetry studies reveal an extension

of π-conjugation that involves the linker and tetrapyrrolic ring of the macrocycle. Such features are rationalized in terms of "push-pull" effects that dominate the electronic interactions between the porphyrin and aldehydic group of the 2-[(4'-formyl)phenyl]ethynyl-5,10,15,20-tetraphenylporphyrin (System A) (6). Additionally, a second system, that is, the 2-[(4'-methyl)phenyl]ethynyl-5,10,15,20-tetraphenylporphyrin (System B), was synthesized to evaluate the effect of the methyl group on the charge delocalization and the push-pull mechanism hypothesis.

Employing our new porphyrin tectons we have also synthesized a new porphyrin-fullerene dyad, in which C_{60} is directly linked to the tetrapyrrolic ring by an ethynylenphenylene subunit. Fluorescence measurements and transient absorption investigations with the newly synthesized donor-acceptor dyad reveal that ultrafast energy and electron transfer processes occur with high quantum yields in non-polar and polar solvents, respectively.

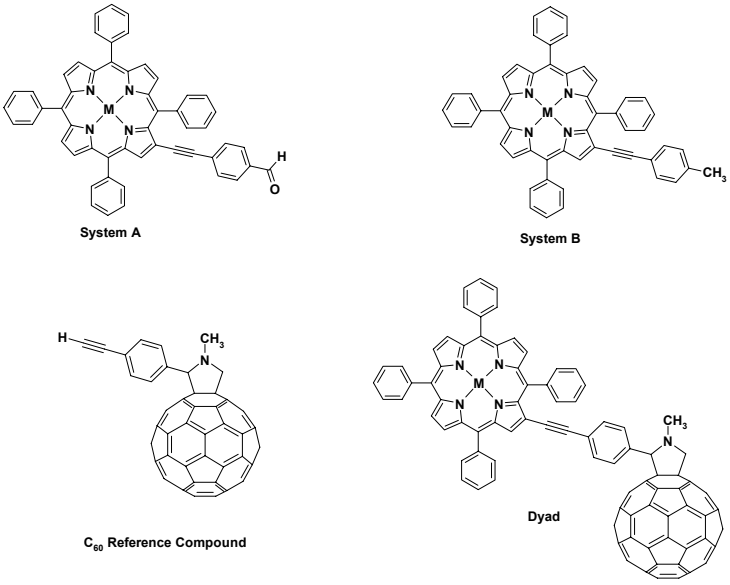

Figure 1. Systems studied, M = 2H, Zn

UV/visible Studies. The UV/vis spectra of all the compounds show interesting characteristics concerning the porphyrin systems. In Table 1 the spectral features of all the new compounds are reported. The spectra of System A and B in toluene, present a broad Soret band, shifted towards higher wavelengths comparing with the Soret band of H_2-TPP (Figure 2). In toluene, the Soret band of System B is located at 428 nm, while that of System A is at 432 nm, with values of the molar extinction coefficients of $2.25 \cdot 10^5$ $M^{-1}cm^{-1}$ and $2.09 \cdot 10^5$ $M^{-1}cm^{-1}$, respectively. H_2P-C_{60} shows the Soret band located at 429 nm, with a molar extinction coefficient of $2.16 \cdot 10^5$ $M^{-1}cm^{-1}$. Furthermore, in this last spectrum a broad band, located between 300 and 350 nm, due to the C_{60} moiety is present. (Figure 3).

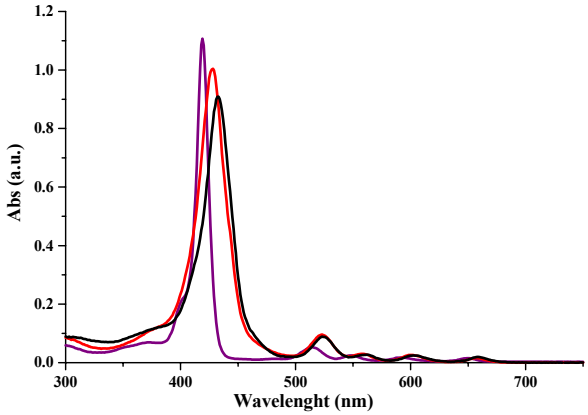

Figure 2. Comparison between H_2-TPP (Purple line), System B (Red line) and System A (Black line) in toluene solution.

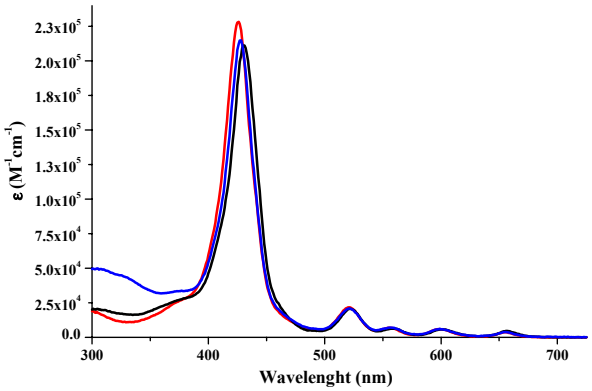

Figure 3. Comparison between H_2P-C_{60} dyad (Blue line), System B (Red line) and System A (Black line) in toluene solution.

In our opinion, the position of the Soret bands and the ε values of such absorptions, compared with those of H_2-TPP, are influenced by the electronic conjugation of the substituents in the β-pyrrole position. The smaller value of ε in the System A derives from the electron-withdrawing effect of the aldehydic group. The extension of conjugation based on the resonance effect also justifies the shift of the Soret band to higher wavelengths if compared with the shift of the band of System B. This observation can be justified by the presence of an electron-donating effect of the porphyrin towards the electron- withdrawing aldehydic group of System A, generating a "push-pull" effect that is transmitted through the carbon-carbon skeleton of the ethynylenphenylen subunit. This effect lowers the electron density of the tetrapyrrole ring and , in turn, lowering the value of ε of System A. On the contrary, in H_2P-C_{60} only an overall electron-withdrawing effect due to the C_{60} moiety can be observed. Furthermore the Q bands of all the examined compounds are slightly shifted. The introduction of zinc into the macrocycles produces an increase in the electron density of the rings giving very similar values of molar extinction coefficients in both porphyrins, $2.38 \cdot 10^5$ $M^{-1}cm^{-1}$ and $2.39 \cdot 10^5$ $M^{-1}cm^{-1}$ for System A and B, respectively, despite the 4 nm difference in the Soret band, 434 nm for System B and 438 nm for System A. The spectra of the free bases and zinc complexes of System B and dyad are virtually superimposable as illustrated in Figure 3

and Figure 4. From the Figure 4 it is also discernable that ZnP-C_{60} spectrum is the sum of the Zn-System B spectrum and of N-methyl-2-(4'-ethynyl)phenyl-3,4-fulleropyrrolidine compound, (C_{60} reference compound) which was synthesized as reference.

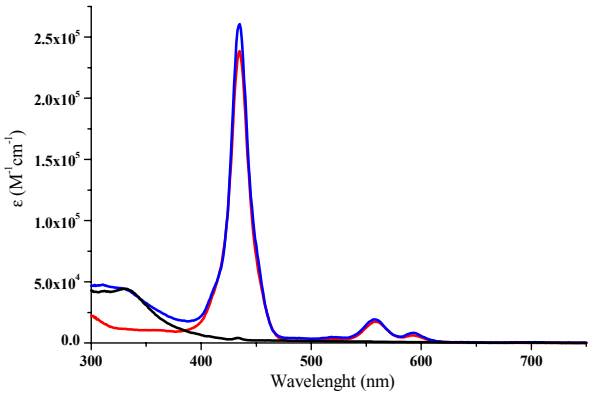

Figure 4. UV/visible spectra in toluene solution of ZnP-C_{60} dyad (Blue line), ZnSystem B (Red line) and C_{60} reference compound (Black line).

TABLE I. UV-visible spectral data of all investigated compounds in Toluene and THF.

Compounds	Toluene. λmax nm (ε·10^{-4})	THF. λmax nm (ε·10^{-4})
System A	311(2.17), 432(20.9), 525(2.03), 560(0.62), 602(0.58), 659(0.46)	428(20.2), 522(1.92), 558(0.59), 601(0.54), 658(0.40)
System B	428(22.5), 523(2.15), 558(0.60), 600(0.59), 657(0.36)	424(20.1), 521(1.89), 556(0.62), 599(0.52), 656(0.32)
H_2P-C_{60}	300(4.88), 429(21.6), 523(2.1), 558(0.71), 601(0.62), 657(0.38)	300(4.6), 425(19.1), 521(1.85), 556(0.65), 600(0.54), 656(0.34)
Zn-System A	311(2.17), 438(23.8), 559(1.86), 596(0.96)	437(22.6), 566(1.72), 603(0.87)
Zn-System B	434(23.9), 558(1.75), 592(0.63)	434(24.7), 564(1.67), 600(0.60)
ZnP-C_{60}	311(4.8), 434(26.1), 558(1.94), 593(0.82)	311(4.5), 435(21.6), 565(1.46), 601(0.62)

^{1}H-NMR Analysis. In the NMR spectra it is possible to observe a further effect of aldehydic group, in fact comparing the β-pyrrole proton signals it is clearly discernable in the System B spectrum, a doublet located at 8.75 ppm, that is fused with singlet at 8.80 ppm in the System A spectrum. Moreover all the proton signals of System A are shifted towards lower field, except the singlet at 8.80 ppm, respect to the proton signals of System B (Figure 5).

Figure 5. ^{1}H-NMR β-pyrrole proton pattern of System A (a) and System B (b).

It is possible to explain this observation assuming the presence of an extention of conjugation starting from the tetrapyrrole ring and arriving at the aldehydic group through the β-substituent; so changing the substituent on the phenyl ring linked to the β-position a shift towards lower frequencies is evident when going from a methyl to an aldehydic group.

Finally it should be noted that the β-pyrrole proton pattern in the ^{1}H-NMR spectrum of the free base porphyrin-fullerene dyad is completely similar to that of System B. The ^{1}H-NMR spectra of the corresponding zinc derivatives present identical β-pyrrole proton pattern (Figure 6), this aspect seems to evidence the fact that the metal insertion makes equal in terms of β-pyrrole proton resonancies all the system studied: Zn-System A, Zn-System B and Zn-Porphyrin-Fullerene Dyad.

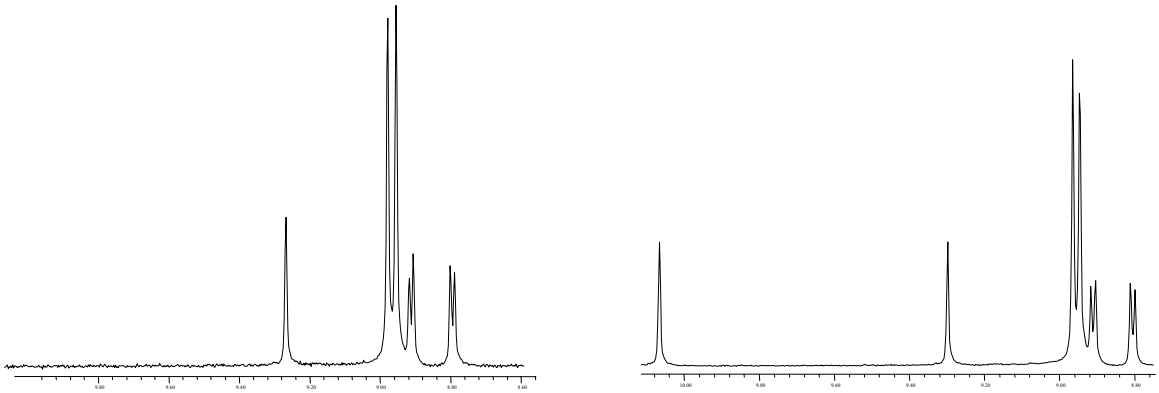

Figure 6. ^{1}H-NMR β-pyrrole proton pattern of Zn-Dyad (a) and Zn-System A (b).

Cyclic Voltammetry Studies. The cyclic voltammograms, in DCB (solvent), with $TBAPF_6$ (supporting electrolyte), reveal the influence of the beta substituent on the oxidation potentials of the porphyrins. In fact the free base porphyrins of System A and System B are characterized by two reversible oxidation processes centered at 1.10, 1.43 and 1.08, 1.44 V respectively, while in general H_2-TPP shows two reversible oxidations at 1.05 and 1.48 V (7).

The two systems also present two reversible reductions centered at -1.10 and -1.34 volts for the System A and –1.16 and –1.44 volts for the System B. The difference of 60 and

100 mV respectively for the first and second reduction potential between the two systems reflects the electron-withdrawing effect (8) of the aldehydic group of the System A. The zinc derivatives of both the systems show two reversible oxidations at 0.95 and 1.21 V for System A and 0.93 and 1.17 V for System B, while it is possible to detect only one reversible reduction for both the compounds at -1.28 and -1.33 respectively. From the reported data, it is evident that the HOMO-LUMO gap of the porphyrin systems is lowered going from H_2-TPP, 2.29 V to System B and System A, 2.24 and 2.20 V respectively. Such observation is justified by postulating an extension of conjugation along the linker (Figure 7).

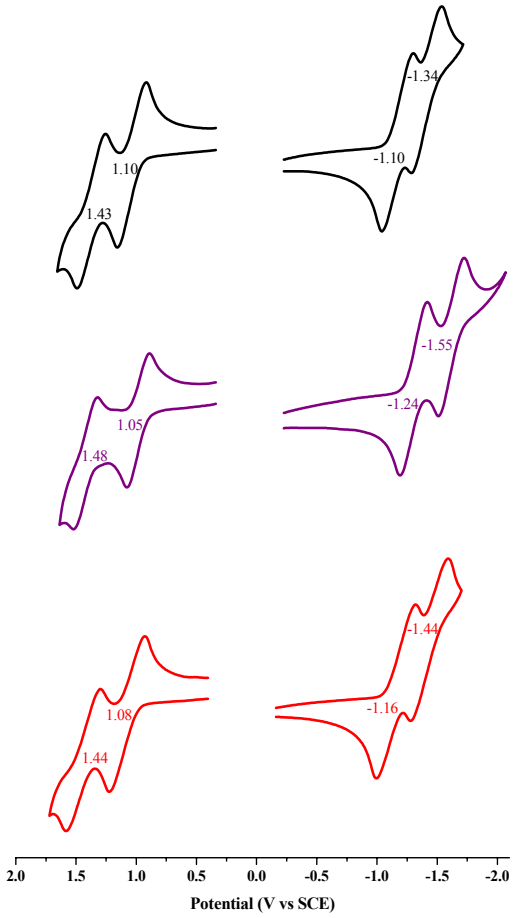

Figure 7. Cyclic voltammograms of H_2-TPP (Purple line), System A (Black line) and System B (Red line) in o-DCB, 0.05 M $TBAPF_6$.

In figure 8 are depicted the cyclic voltammograms of System B, free base porphyrin-fullerene dyad and C_{60} reference compound. Taking in to the consideration the potential values both for the oxidation and reduction processes of the three compounds, we can assume that in the dyad the porphyrin and fullerene chromophores could be considered as non interacting unit, retaining their own electronic and physical properties.

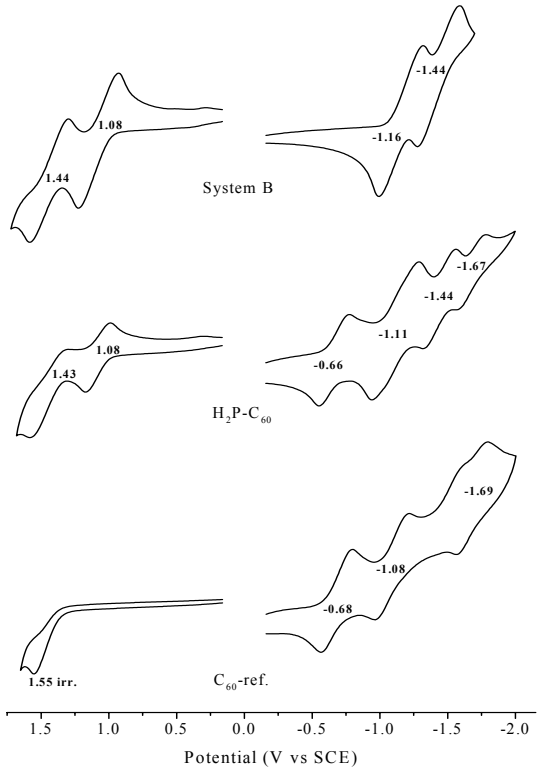

Figure 8. Cyclic Voltammograms of System B, free base porphyrin-fullerene dyad (H_2P-C_{60}) and C_{60} reference compound (C_{60}-ref.).

Photophysical Studies. Steady state fluorescence spectra were recorded to analyze the photophysical properties of the new porphyrins and dyads. The fluorescence steady state studies were recorded in two different solvents: toluene and THF. The excitation wavelength was 525 nm for the free base derivatives and 560 nm for the zinc derivatives. In toluene, System A presents two emission bands at 666 and 734 nm, while System B at 663 nm and 731 nm. Such difference of 3 nm remains also in THF. In the corresponding zinc derivatives the emission maxima are located at 607 and 661 nm for Zn-System A, while they are at 605 and 658 nm for Zn-System B.

Steady state fluorescence spectra of zinc derivatives in THF show a substantial red shift due to the coordinating effect of the solvent. In fact in THF the first emission maximum of Zn-System A is at 620 nm.

In toluene solution, the fluorescence of the porphyrin part in H_2P-C_{60} is 93% quenched by the C_{60} moiety. The fluorescence quenching is calculated taking System B as reference. On the other hand, for ZnP-C_{60} the quenching is 99%. In addition to the higher quenching of the porphyrin fluorescence, in the spectra of the ZnP-C_{60} a third emission band appears at 715 nm (Figure 9). An excitation spectrum collected at 715 nm(*i.e.*, exciting from 400 to 650 nm) confirms that the origin of this emission band is the porphyrin moiety. Further analysis on the reference compound N-methyl-2-(4'-ethynyl)phenyl-3,4-fulleropyrrolidine identifies this band as the singlet excited state emission of C_{60} (Figure 10).

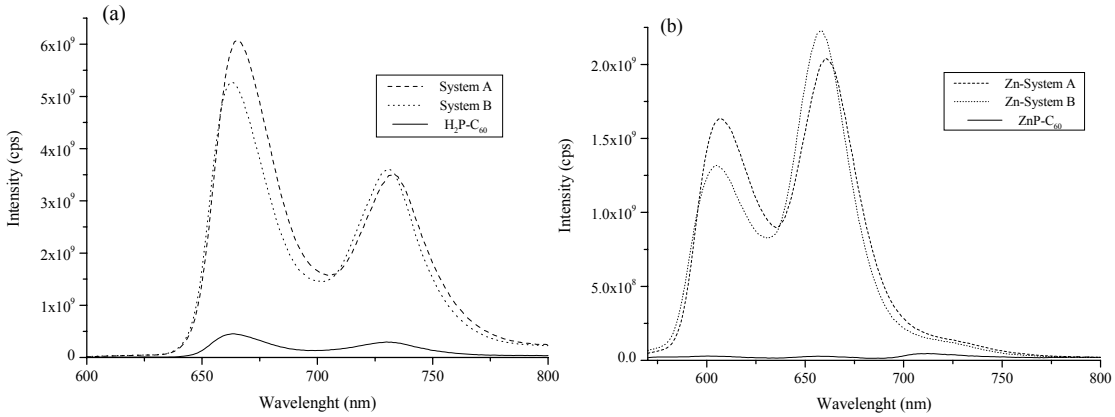

Figure 9. Steady state fluorescence spectra of System A, System B and H_2P-C_{60}, (a) and corresponding zinc derivatives (b) in toluene solution, respectively upon excitation at 525 nm and 560 nm.

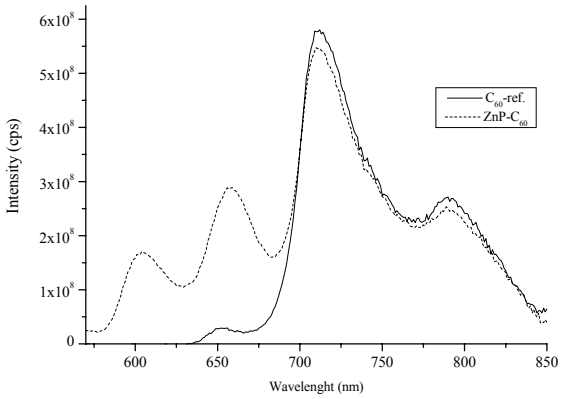

Figure 10. Steady state fluorescence spectra of C_{60}-ref. and ZnP-C_{60} in toluene solution upon excitation at 400 nm. The relative absorbance match (0.05 a.u.) at excitation wavelength.

Such data demonstrate that in toluene solution the principal deactivation pathway of the porphyrin fluorescence is a near quantitative energy transfer from the singlet excited state of zinc porphyrin to the singlet excited state of C_{60}. In THF the porphyrin fluorescence quenching in H_2P-C_{60} is much stronger compared to what has been seen in toluene. In ZnP-C_{60} fluorescence spectra, on the other hand, we do not observe the fluorescence emission of $^{1*}C_{60}$ at 715 nm.

Femtosecond transient absorption spectroscopy was used to complement the aforementioned fluorescence experiments. In particular, the references (i.e., Zn-System B and System B) and the electron donor-acceptor dyads (i.e., ZnP-C_{60} and H_2P-C_{60}) were probed upon 387 nm excitation. This guarantees the predominant photoexcitation of the Zn porphyrin and free base porphyrin chromophores. At first our attention should be directed to the references. For System B, for example, we observe the nearly instantaneous formation of the singlet excited state – only a fast internal conversion (i.e.,

~ 2 ps) from an higher lying excited state precedes the singlet excited state formation – for which we gather the following spectral characteristics: minima at 521, 557, 600 and 660 nm and a maximum in the near infrared at 700 nm. The minima correspond to maxima seen in the System B ground state absorption spectrum. Similar ground state bleachings (i.e., 555 and 595 nm) and new maxima in the near infrared (i.e., 710 nm) were noted for Zn-System B. In contrast, the singlet excited state lifetimes of System B (i.e., 10.5 ns) and Zn-System B (i.e., 2.3 ns) mainly differ.

The same singlet excited state formations of Zn-System B and System B were registered in ZnP-C_{60} and H_2P-C_{60}, respectively, despite the presence of the electron accepting C_{60}. This fact affirms the successful photoexcitation of the chromophores in the electron donor-acceptor dyads in toluene and THF. At longer delay times, however, the electron donor-acceptor dyads revealed a behavior that is vastly different from the reference systems. In particular, ultrafast deactivations of the singlet excited state are derived from kinetic analyses of the ZnP-C_{60} (i.e., toluene: 15.9 ps; THF: 5.8 ps) and H_2P-C_{60} (i.e., toluene: 20.5 ps; THF: 50.7 ps) transient species in the different solvents – see Figures 13-15.

Spectral characteristics, which are taken immediately at the conclusion of the Zn-Sytem B and System B singlet excited state decays, bear no resemblance with the singlet or triplet features of either chromophore. On the contrary in toluene the distinct absorption of the C_{60} singlet excited state evolve around 900 nm – see Figure 11 – within the first 100 ps – with kinetics (i.e., ZnP-C_{60}: 17.4 ps; H_2P-C_{60}: 23 ps) that resemble the Zn-System B or System B singlet deactivations.

Therefore, we postulate that in toluene a transduction of singlet excited state energy is responsible for the kinetic and spectral observations. On the longer time scale, namely, up to 1500 ns the C_{60} singlet / C_{60} triplet intersystem crossing takes place, which leads ultimately to the quantitative triplet formation, which is spectroscopically confirmed by the growth of a new transient that maximizes at 700 nm. In THF, on the other hand, it is not the C_{60} singlet feature in the near infrared that is seen for both electron donor-acceptor dyads, but the C_{60} radical anion bands, as gathered in Figure 12 and 13, with maxima at 1000 nm.

The C_{60} radical anion band in the near infrared is complemented by the Zn-System B and System B radical cation absorptions in the visible with transient maxima at 635 and 690 nm, respectively. Both, the radical cation and the radical anion features are formed with the same kinetics, which leads us to conclude that in THF an intramolecular electron transfer converts the initial excited state into a radical ion pair state. Moreover, the radical cation and radical anion transitions also decay with the same kinetics. From the corresponding decay dynamics we derive lifetimes of the radical ion pair states of 398 and 1175 ps for the ZnP-C_{60} and H_2P-C_{60}, respectively. The different charge recombination dynamics (i.e., 2.5 x 10^9 s^{-1} versus 8.5 x 10^8 s^{-1}) are well in line with kinetics that are located in the inverted region of the parabolic dependence of electron transfer rate on the thermodynamic driving force.

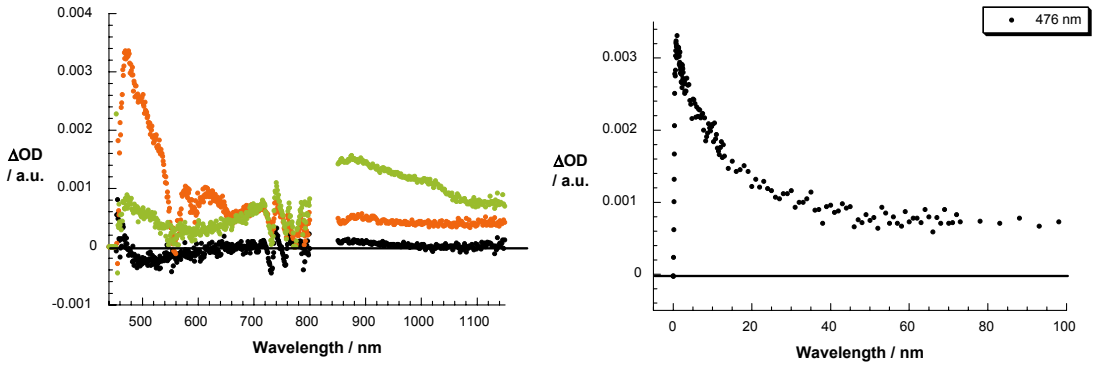

Figure 11: On the left – differential absorption spectra (visible and near infrared) obtained upon femtosecond flash photolysis (387 nm) of ZnP-C_{60} (ca. 1.0×10^{-6} M) in toluene with 0.05, 1.4 and 50 ps time delays at room temperature. On the right – time-absorption profile of the spectra shown above at 476 nm, reflecting the intramolecular energy transfer dynamics.

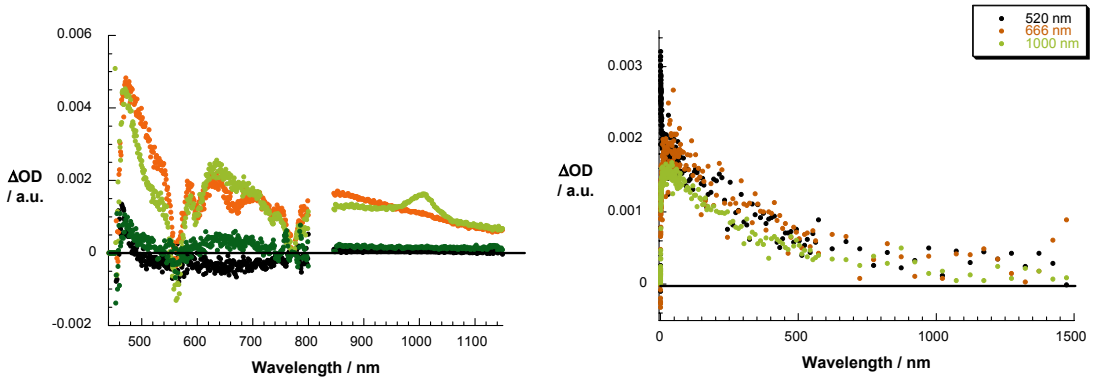

Figure 12: On the left – differential absorption spectra (visible and near infrared) obtained upon femtosecond flash photolysis (387 nm) of ZnP-C_{60} (ca. 1.0×10^{-6} M) in THF with 0.05, 1.4, 50 and 1525 ps time delays at room temperature. On the right – time-absorption profile of the spectra shown above at 520, 666 and 1000 nm, reflecting the intramolecular charge separation and charge recombination dynamics.

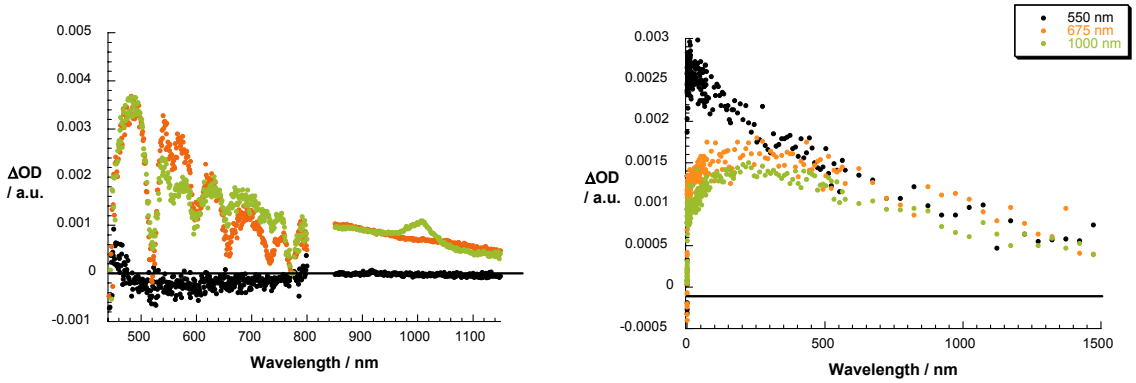

Figure 13: On the left– differential absorption spectra (visible and near infrared) obtained upon femtosecond flash photolysis (387 nm) of H_2P-C_{60} (ca. 1.0×10^{-6} M) in THF with 0.05, 1.4 and 200 ps time delays at room temperature. On the right – time-absorption profile of the spectra shown above at 550, 675 and 1000 nm, reflecting the intramolecular charge separation and charge recombination dynamics.

Conclusion. Two new β-ethynyl porphyrins were synthesized and the substituent effect has been studied. The new compounds show an extension of conjugation along the β-substituent, that leads to a "push-pull" effect when aldehydic group is present on the phenyl ring of the substituent. These aspects are outlined by UV-vis, NMR and cyclic voltammetry studies. Although the substituent affects the fundamental state properties of the porphyrins, it has been shown that beta substitution on the pyrrole ring deeply affects the physico-chemical properties of the porphyrins, giving us a further tool to modulate porphyrin-fullerene interaction in the electron donor-acceptor systems. The new porphyrin-fullerene dyad presents moderate charge separation state lifetime that could be improved by increasing the porphyrin-fullerene distance. This prompts us the opportunity to study the "photonic wire" behaviour of an enlarged spacer.

Acknowledgments

The financial support from the Italian MIUR for a PhD grant (A.L.), the Deutsche Forschungsgemeinschaft (SFB 583), FCI, The Office of Basic Energy Sciences of the U.S. Department of Energy is gratefully acknowledged. We also thank Giuseppe D'Arcangelo and Alessandro Leoni for their technical assistance and Dr. Marzia Nuccetelli for the MALDI spectra and Dr. Marianna Gallo for NMR Spectra.

References

1. Guldi, D. M. *Chem. Soc. Rev.* **2002**, *31*, 22-36
2. a) D'Souza, F.; Deviprasad, G. L.; Zandler, M. E.; Hoang, V. T.; Klykov, A.; Van Stipdonk, M.; Perera, A.; El-Khouly, M. E.; Fujitsuka, M.; Ito, O. *J. Phys. Chem. A*. **2002**, *106*, 3243-3252 b) Satake, A.; Kobuke, Y. *Tetrahedron*, **2005**, *61*, 13-41
3. a) Choi, M.-S.; Aida, T.; Luo, H.; Araki, Y.; Ito, O. *Angew. Chem. Int. Ed.* **2003**, *42*, 4060-4063 b) Galili, T.; Regov, A.; Levanon, H.; Schuster, D. I.; Guldi, D. M. *J. Phys. Chem. A* **2004**, *108*, 10632-10639
4. a) Imahori, H.; Tamaki, K.; Guldi, D. M.; Luo, C.; Fujitsuka, M.; Ito, O.; Sakata, Y.; Fukuzumi, S. *J. Am. Chem. Soc.* **2001**, *123*, 2607-2617 b) Kodis, G.; Liddell, P. A.; De la Garza, L.; Clausen, P. C.; Lindsey, J. S.; Moore, A. L.; Moore, T. A.; Gust, D. *J. Phys. Chem. A*, **2002**, *106*, 2036-2048
5. a) Reed, C. A.; Drovetskaya, T.; Boyd, P. *Tetrahedron Lett.* **1995**, *36*, 7971-7974 b) Guldi, D. M.; Nuber, B.; Bracher, P. J.; Alabi, C. A.; MacMahon, S.; Kukol, J. W.; Wilson, S. R.; Schuster, D. I. *J. Phys. Chem. A* **2003**, *107*, 3215-3221
6. Meier, H.; Mühling, B.; Kolshorn, H. *Eur. J. Org. Chem.* **2004**, 1033-1042
7. a) Kadish, K. M.; Lindsey J. S. (Kadish, K. M.; Guilard R.; Smith, K. M. eds) *Handbook of Porphyrins and Phthalocyanine* Vol.9; b) Autret, M.; Ou, Z.; Antonini, A.; Boschi, T.; Tagliatesta, P.; Kadish, K. M. *J. Chem. Soc. Dalton Trans.* **1996** 2793-2797; c) Kadish, K. M.; Guo, N.; Van Caemelbecke, E.; Froiio, A.; Paolesse, R.; Monti, D.; Tagliatesa, P.; Boschi, T.; Prodi, L.; Bolletta, F.; Zaccheroni, N. *Inorg. Chem.* **1998**, *vol.37*, *10*, 2358-2365.

8. a) D'Souza, F.; Zandler, M. E.; Tagliatesta, P.; Ou, Z.; Shao, J.; Van Caemelbecke, E.; Kadish, K. M. *Inorg. Chem.* **1998**, *37*, 4567-4572; b) Kadish, K. M.; D'Souza, F.; Villard, A.; Autret, M.; Van Caemelbecke, E. ; Blanco, P.; Antonini, A.; Tagliatesta, P. *Inorg. Chem.* **1994**, *33*, 5169-5170. c) Binstead, R. A.; Crossley, M. J.; Hush, N. J. *Inorg. Chem.* **1991**, *30*, 1259-1264.